

PSNR BASED OPTIMIZATION APPLIED TO ALGEBRAIC RECONSTRUCTION TECHNIQUE FOR IMAGE RECONSTRUCTION ON A MULTI-CORE SYSTEM

A. Bharathi Lakshmi¹ and D. Christopher Durairaj²

¹Department of Information Technology, Assistant Professor, Affiliated to Madurai Kamaraj University, Virudhunagar, 626001, India.

²Research center in Computer Science, VHNSNC, Virudhunagar, 626001, India.

E-mail: bharathilakshmi.a@gmail.com, kesterkaren@gmail.com

Abstract

The present work attempts to reveal a parallel Algebraic Reconstruction Technique (pART) to reduce the computational speed of reconstructing artifact-free images from projections. ART is an iterative algorithm well known to reconstruct artifact-free images with limited number of projections. In this work, a novel idea has been focused on to optimize the number of iterations mandatory based on Peak to Signal Noise Ratio (PSNR) to reconstruct an image. However, it suffers of worst computation speed. Hence, an attempt is made to reduce the computation time by running iterative algorithm on a multi-core parallel environment. The execution times are computed for both serial and parallel implementations of ART using different projection data, and, tabulated for comparison. The experimental results demonstrate that the parallel computing environment provides a source of high computational power leading to obtain reconstructed image instantaneously.

Keywords: *Image Processing, Image Reconstruction, Iterative Image Reconstruction, Algebraic Reconstruction Technique, Parallel Processing, OpenMP*

Abstrak

Pekerjaan saat ini mencoba untuk mengungkapkan Teknik Rekonstruksi Algebraic paralel (pART) untuk mengurangi kecepatan komputasi untuk merekonstruksi gambar bebas artefak dari proyeksi. ART adalah algoritma iteratif yang dikenal untuk merekonstruksi gambar bebas artefak dengan jumlah proyeksi yang terbatas. Dalam karya ini, sebuah gagasan baru difokuskan untuk mengoptimalkan jumlah iterasi yang wajib berdasarkan Peak to Signal Noise Ratio (PSNR) untuk merekonstruksi gambar. Namun, ia menderita kecepatan perhitungan terburuk. Oleh karena itu, upaya dilakukan untuk mengurangi waktu komputasi dengan menjalankan algoritma iteratif pada lingkungan paralel multi-core. Waktu eksekusi dihitung untuk penerapan ART secara serial dan paralel dengan menggunakan data proyeksi yang berbeda, dan, ditabulasikan sebagai perbandingan. Hasil percobaan menunjukkan bahwa lingkungan komputasi paralel menyediakan sumber daya komputasi tinggi yang menghasilkan gambar yang direkonstruksi seketika.

Kata Kunci: *Pemrosesan gambar, rekonstruksi gambar, rekonstruksi gambar iteratif, teknik rekonstruksi aljabar, pemrosesan paralel, OpenMP*

1. Introduction

Image reconstruction methods are central to many of the new applications of medical imaging such as Positron Emission Tomography (PET), Computed Tomography (CT), Magnetic Resonance Imaging (MRI) and Electron Magnetic Resonance Imaging (EMRI). They are most commonly used to visualize detailed internal structure and limited function of the object of interest.

Image reconstruction is a mathematical process that generates images from projection data acquired at many different angles around the object of interest. The projections are collected by sweeping the magnetic field at projection angles defined by the magnetic field gradient directions

[1, 2]. To perform image reconstruction, the projections $p_{\theta}(r)$, collected along a set of field-gradient orientations in polar coordinates, are used to obtain the image $f(x, y)$ [3] as given in the equation(1).

$$\begin{aligned} f(x, y) &= \int_0^{\pi} P_{\theta}^*(r) d\theta \\ &= \int_0^{\pi} \left[\int_{-\infty}^{\infty} P_{\theta}(k) |k| e^{-2\pi i k r} - dk \right] d\theta \end{aligned} \quad (1)$$

Here r is taken on the x-y plane such that $r = x \cos \theta + y \sin \theta$, and $p_{\theta}^*(r)$ is the projection $p_{\theta}(r)$

filter according to the expression inside the square brackets [3].

Image reconstruction has been carried out using different types of reconstruction algorithms [4, 1]. Reconstruction methods utilize projection data as input and generate the estimate that resembles the internal structure as output [5, 6]. Data sets with 36 projections measured from 0^0 to 180^0 around the phantom object were considered in the present study. The same data set was used for testing the capability of the algorithms from restricted number of projections, by skipping projections at uniform angular distribution.

Reconstruction of images is usually done in two ways: Analytical and Iterative. Analytical method such as Back Projection (BP) or Filtered Back Projection (FBP) is used for different imaging modalities such as CT and PET in clinical settings because of its speed and easy implementation [3]. For noisy projection data as well as for limited number of projections, the FBP method of image reconstruction shows very poor performance. Hence currently there is considerable interest to evaluate the use of other reconstruction methods for medical imaging techniques [6]. FBP algorithm produces high-quality images with excellent computational efficiency. However, FBP produces low Signal-to-Noise Ratio (SNR) images when limited number of projections is used [12].

An Iterative method using a non-linear fit to the projection data has shown to give ripple free images [7]. Iterative Methods are based on optimization strategies incorporating specific constraints about the object and the reconstruction process. The iterative reconstruction techniques perform better than the FBP method when reconstruction is attempted with limited number of projection data [3]. Some of the accepted iterative algorithms are Additive Algebraic Reconstruction Technique (AART) and Multiplicative Algebraic Techniques (MART) [12].

However, the quality of the reconstructed images obtained from AART algorithm depends on number of iterations. Based on the number of available number of projections and the size of the phantom, the number of iterations differs. It is therefore necessary to find the best iteration in order to exploit correctly the promising iteration based on a better Peak to Signal Noise Ratio (PSNR) of the reconstructed images. Based on the equation(1) an optimization program has been developed for the given data set. The best PSNR value is obtained and verified whether the same PSNR value is achieved even after the selected iteration.

Parallel computing is emerging as a principle

theory in high performance computing [14]. In recent years, parallel computing with massive data has emerged as a key technology in imaging techniques also. Shared memory parallelization has been proved to be a best way to attain better runtime performance recently for image reconstruction [15]. A shared-memory multiprocessor (SMP) consists of a number of processors accessing one or more shared memory modules. The penalty of using inter-processor communication is not up to the mark on SMP compared to distributed memory architectures [15]. For a relatively large data size, it is advantageous to use SMP architecture. It has also been shown that shared memory parallelization is more suitable than distributed memory parallelization for image processing tasks and leads to better throughput as most of the computers now have two or more processors which share the memory [16]. These features have motivated us to perform the parallelization of Algebraic Reconstruction Technique (ART) on a SMP parallel architecture.

The present study focuses on reducing the computational complexity of ART using parallel programming techniques. Section 2 describes about ART briefly. The design and implementation ART algorithm in both parallel and sequential version are given in section 3 Section 4 discusses the results.

2. Methods

Radon Transformation

The main application of image reconstruction from projection technique is mostly related to medical image processing. The Procedure to implement Image Reconstruction from Projection (IRP) technique in the practical applications are “scanning” or “data acquisition” is considered to be the first and the very important step [17]. Such data acquisition is done by means of PET, CT, MRI or EMRI in a procedure by passing rays in specific intervals of angles.

The Radon Transformation is a fundamental tool that computes projections of an image matrix along specified directions [18]. The 2D Radon transformation is the projection of the image density along a radial line oriented at a specific angle. The value of a 2-D function at an arbitrary point is uniquely obtained by the integrals along the lines of all directions passing the point. The Radon transformation shows the relationship between the 2-D object and its projections. Figure 1 shows a 2-D function $f(x, y)$. Integrating along the line, whose normal vector is in θ direction on s axis results in the $g(s, \theta)$ projection represented in

equation(2). The points on the line whose normal vector is in θ direction and passes the origin of (x, y) -coordinate satisfy the equation $x\cos\theta + y\sin\theta = 0$. The general equation of the radon transform is acquired as

$$g(s, \theta) = \iint f(x, y) \cdot \delta(x\cos\theta + y\sin\theta - s) dx dy \quad (2)$$

where δ is zero for every argument except to 0 and its integral is one [19].

The projection data obtained thus from Radon Transformation is utilized as input by the Reconstruction algorithm that produce estimates of the original internal structure as output [5, 20]. The size of data sets acquired by the different imaging modalities are usually huge because of the complex data type of the raw collection data, multiple gradients in the experiments, high dimensions of the resultant 3-D images, higher k-space requirement of whole body imaging and the number of points collected from the imager. The iterative methods, hence, suffers more reconstruction time.

Algebraic Reconstruction Technique (ART)

Image reconstructions based on Iterative methods create two-dimensional images from scattered or incomplete projections such as the radiation readings acquired during a medical imaging study. Algebraic Reconstruction Technique (ART) falls under the category of Iterative methods.

ART is one of the methods used for solving the linear system which appears in image reconstruction. ART can be broadly classified as either sequential or simultaneous or block iterative [21]. ART is a fully sequential method and has a long history and literature. Originally it was

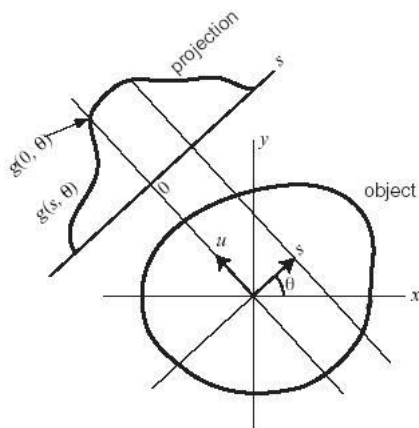


Figure. 1. The Radon Transform computation

proposed by Kaczmarz [22], and independently, for use in image reconstruction by Gordan, Bender and Herman [23]. The vector of unknowns is updated at each equation of the system, after which the next equation is addressed. If system of equation is (0.1) consistent, ART converges to a solution of this system. If the system is inconsistent, every subsequence of cycles through the system converges, but not necessarily to a least square solution [24].

ART perform corrections during iterations, without increasing the computation time. The image $f(x, y)$ is a continuous two dimensional function and an infinite number of projections are mandatory for reconstruction [12]. In practice $f(x, y)$ is calculated using a finite number of points f_j ($j = 1, 2, 3, \dots, N$) where N represents the total number of cells, from a finite number of projections as shown in figure. 2.

In figure 2 a ray is a fat line running through the (x, y) -plane where each ray is of width r . A line integral is called a ray-sum represented as p_i measured with i^{th} ray as shown in figure. 2.

The relationship between the f_j 's and p_i 's may be expressed as

$$\sum_{j=1}^N w_{ij} f_j = p_i, \quad i = 1, 2, \dots, M \quad (3)$$

where M is the total number of rays (in all the projections) and w_{ij} is the weighting factor that represents the contribution of the j^{th} cell to the i^{th} ray integral and p_j represents a set of matrix equation for the data point f_j .

The expanded form for equation(3) for the j^{th} sample is given by

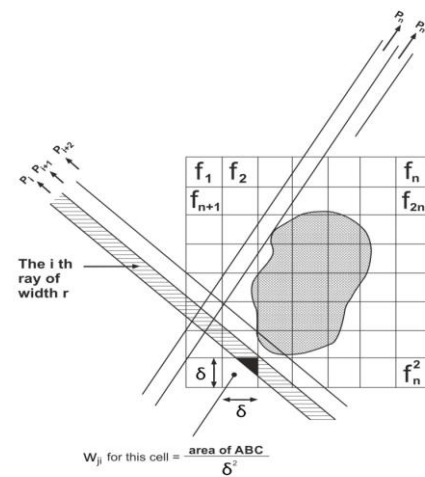


Figure. 2. Representation of an image projected on i^{th} ray.

$$\begin{aligned}
w_{11}f_1 + w_{12}f_2 + w_{13}f_3 + \dots + w_{1N}f_N &= p_1 \\
w_{21}f_1 + w_{22}f_2 + w_{23}f_3 + \dots + w_{2N}f_N &= p_2 \\
&\vdots \\
w_{M1}f_1 + w_{M2}f_2 + w_{M3}f_3 + \dots &+ w_{MN}f_N = p_M
\end{aligned} \quad (4)$$

Equation(4) can also be expressed in the form of algebraic equations as

$$\begin{aligned}
P_j &= W_{1j}f_1 + W_{2j}f_2 \\
&\quad + W_{3j}f_3 + \dots + W_{nj}f_n \\
P_j &= \sum_{j=1}^N W_{ij}f_j \quad i = 1, 2, \dots, M \quad (5)
\end{aligned}$$

Here, W_{ij} is the weighting factor that represents the contribution of the j^{th} cell to the j^{th} sample sum and P_j represents a set of matrix equations for the data point f_j . Most of the w_{ij} in Eqn. 4 is zero since only a small number of cells contribute to any given ray-sum. The density values f_j are iteratively adjusted until the calculated projections agree with the measured projections [12]. Each projected density is thrown back across the reconstruction space in which the densities are iteratively modified to bring each reconstructed projection into concur with the measured projection [25]. The projection data set is sustained in a vector and a weight sparse matrix w_{ij} is constructed. Every row in w_{ij} sparse matrix may contain $m + n - 1$ (where $m \times n$ is the resolution). As every row stands for the length of the segments obtained by the intersection of ray with the grid, and all reconstruction algorithms use rows of sparse matrix, the best method to store this matrix is in compressed row storage [17].

For each sample, the correction coefficient is computed as: $\alpha_i = \sum_{j=1}^N W_{ij}^2$. The average value of the correction coefficient is calculated. Correction is applied for each cell j as given: $f_i^{l-1} + \lambda \Delta P_j$, where λ is the relaxation parameter. This procedure is iteratively performed for all of the projection angles. As the size of the data set increases, the computation time increases.

OpenMP Architecture and Directives

Parallel computing is a form of computation in which many calculations are carried out simultaneously; large problems are divided into smaller ones, solved concurrently. The parallelism can be

applied in image processing applications by three main ways: 1) Data Parallel 2) Task Parallel and 3) Pipeline Parallel. In Data Parallel approach, the data is divided and distributed among the computing units. The data parallelism to image data can be applied using one of three basic ways: i) Pixel Parallel ii) Row or Column parallel and iii) Block Parallel [27]. This algorithm is parallelized in row/column parallel. In task parallel, image processing instructions/low level operations are grouped into tasks and each task is assigned to a different computational unit. If image processing application requires multiple images to be processed, then pipeline processing of images can be done [28].

pART is implemented using OpenMP parallel computing in C language. OpenMP is a programming model for SMP computer systems. Data in memory can either be shared between all threads or private for one thread. Data transfer between threads is transparent to the programmer. OpenMP uses fork-and-join model of parallel execution. The program written with OpenMP begins execution as a single-process, called the master thread. The master thread executes the current program sequentially until it bump into parallel directives such as #pragma omp. The master thread forks a number of worker threads when it enters a parallel region. A parallel region is a block of code that is executed by all threads concurrently.

The ‘‘parallel for’’ or ‘‘for’’ is a work sharing directive that distributes the workload of a ‘‘for’’ loop among all the threads. Data sharing of variables is mentioned at the beginning of the parallel region or work sharing construct using the SHARED or PRIVATE Clauses.

Data Set

The reconstruction system uses Shepp Logan phantom data of different sizes such as 64, 128 and 256. The figure. 3(a), figure. 3(b), figure. 3(c) shows the Shepp Logan phantom image of 64x64, 128x128 and 256x256 sizes respectively.

The projection data of the phantom images



Figure. 3. The Shepp Logan Phantom Image of size (a)64x64 (b)128x128 (c) 256x256

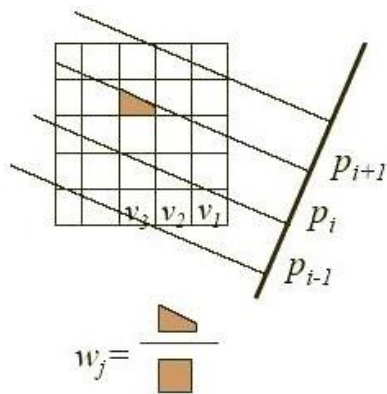


Figure 4. Displays the projected data

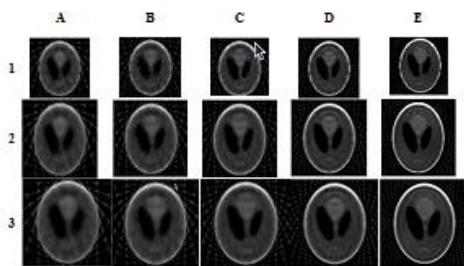


Figure 5. The projection of Shepp Logan Phantom Image. Rows 1, 2 and 3 refer to the 64x64, 128x128, 256x256 data respectively. Columns A, B, C, D and E refer to the 10, 12, 15, 20 and 30 projection taken in 18, 15, 12, 9 and 6 angles respectively.

```

art()
{
  if ( not yet reached all the projections)
  {
    for (all elements in the projection)
    {
      calculate the value by multiplying
      the vector and the calculated data
      in the corresponding
      projection
    }
    calculate the error by subtracting
    the measured data from the calculated
    value
    for(all the rows)
    {
      correct the error by multiplying
      the difference with the
      calculated data.
      apply the corrected value to the
      vector.
    }
  }
  recursively call art function for
  remaining projections
}
    
```

Figure 6. Art algorithm

are obtained using Radon function available in MATLAB. figure 4 shows the projection of the ray passed at a specific angle. The projection of a two dimensional function $f(x,y)$ is a set of line integrals Eqn. (1). The $f(x,y)$ is transferred to a row vector. The rays p_i passed at a specified angle

```

part()
{
  if ( not yet reached all the
      projections)
  {
    omp_set_num_threads(number_of_threa
                        ds);
    #pragma omp parallel for
      shared(elements) private(index)
      schedule(dynamic, num_elements)

    for (all elements in the
        projection)
    {
      omp_set_num_threads(number_of_
                          threads);
      #pragma omp parallel for
        shared(elements) private(index)
        schedule(dynamic, num_elements)
        reduction(+:calculated value)

      calculate the value by
      multiplying the vector and
      the calculated data in the
      corresponding projection
    }

    calculate the error by subtracting
    the measured data from the calculated
    value

    omp_set_num_threads(number_of_threads
                        );

    #pragma omp parallel for
      shared(elements) private(index)
      schedule(dynamic,num_elements)

    for(all the rows)
    {
      correct the error by multiplying
      the difference with the
      calculated data.

      apply the correction.
    }
  }

  recursively call part function for
  remaining projections
}
    
```

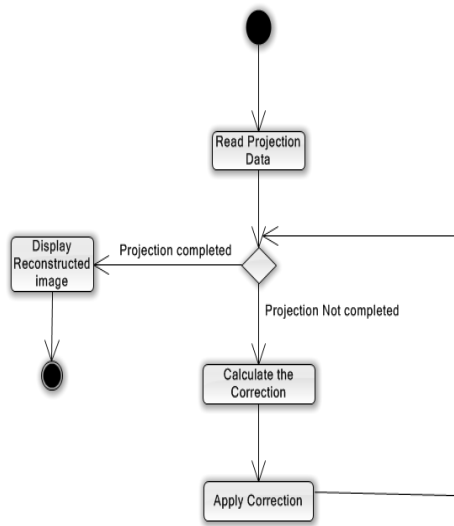
Figure 7. pArt algorithm

collects data by calculating the weight matrix.

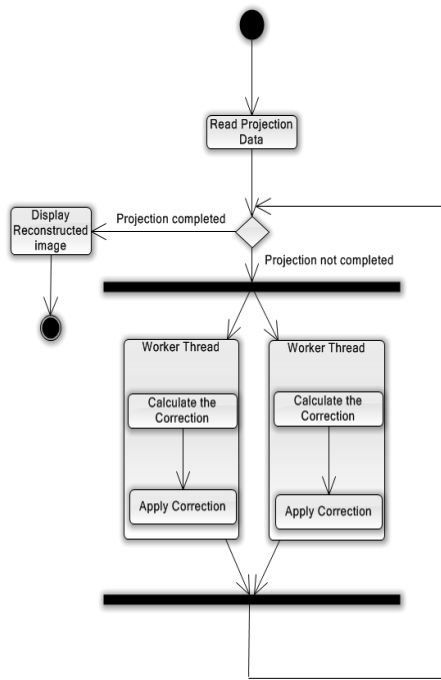
The projections of the Shepp Logan phantom in various angles are plotted in the figure 5. This is obtained by using *radon* function in matlab passing at which specific angles the object should be rotated. This system uses five different angles, such as 6^0 , 9^0 , 12^0 , 15^0 , 18^0 obtaining 30, 20, 15, 12, 10 numbers of projections respectively. Rows 1, 2 and 3 of figure. 5 refer to the projections taken from the images sizes 64x64, 128x128 and 256x256 respectively. Columns A, B, C, D, E refer to the 10, 12, 15, 20 and 30 projections taken in 18, 15, 12, 9 and 6 angles respectively.

Pseudo Code

The pseudo code for ART algorithm implemented



(a)



(b)

Figure 8. UML Activity for reconstructing an image using ART. (a) Sequentially (b) Parallel

in MEX function executed sequentially is given in figure 6.

The pseudo code for pART algorithm implemented in MEX function executed parallel shows in figure 7.

UML Diagram

The operation of ART in sequential and parallel is symbolised in the figure 8(a) and figure 8(b) respectively. Parallel activity is pictured as Fork

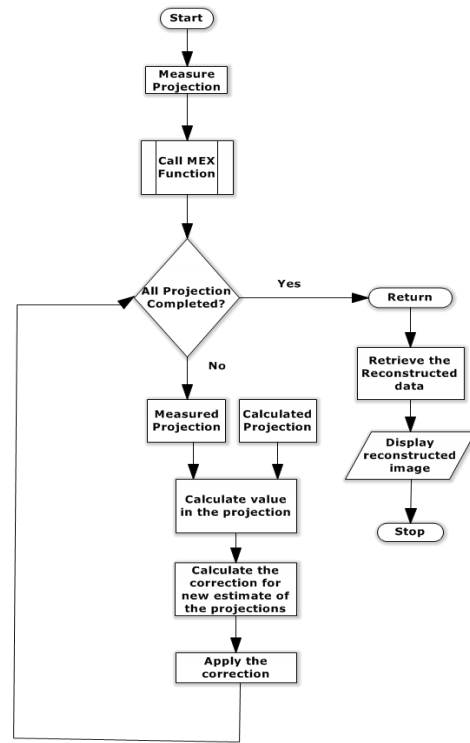


Figure 9: Flow chart for reconstructing an image using ART.

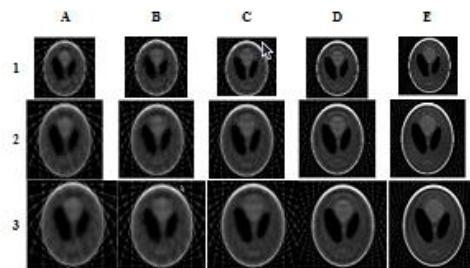


Figure 10. The Reconstructed Shepp Logan Phantom. Rows 1, 2 and 3 refer to the 64x64, 128x128, 256x256 size of the Image respectively. Columns A, B, C, D and E refer to the reconstructed image from the 10, 12, 15, 20 and 30 projections of an image taken in 18, 15, 12, 9 and 6 angles in Sequential and parallel.

and Join.

The data is read from the corresponding number of projections. This data is supplied into the MEX function to execute under single and multiple processors. For each projection the error value is calculated and the correction is applied

Initially, the program starts with initialization at each core. Then the calculated and measured projection data is co-distributed between the workers. After that, each worker calculates the correction and applies the correction as per the algorithm till all the projections are completed. Then the processed data is collected in a vector

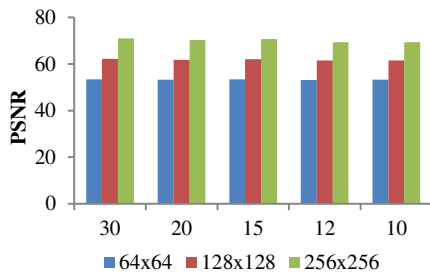


Figure. 11. Plotted the PSNR value obtained while reconstructing Shepp Logan Phantom Images on 64x64, 128x128 and 256x256 sizes using 30, 20, 15, 12 and 10 number of projections.

TABLE 1
PSNR VALUE IN DB FOR THE RECONSTRUCTED SHEPP LOGAN PHANTOM IN SINGLE CORE AND MULTI-CORE ENVIRONMENT

Projections/ Sizes	30	20	15	12	10
64x64	53.3	53.2	53.4	53.1	53.2
128x128	62.1	61.7	62.0	61.4	61.4
256x256	71.0	70.3	70.6	69.3	69.3

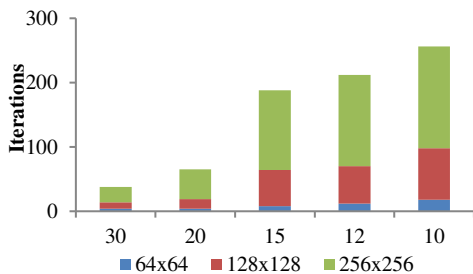


Figure. 12. Optimized number of iteration mandatory to reconstruct Shepp Logan Phantom Images on 64x64, 128x128 and 256x256 sizes using 30, 20, 15, 12 and 10 number of projections.

when the parallelism ends.

3. Results and Analysis

The results of constructing Shepp Logan Phantom image using ART in both sequential and parallel is given in figure 10. In this work, the time complexity of the phantom image of different size (64, 128 and 256) is compared in 2, 4 and 8 cores.

Peak-signal-to-noise ratio (PSNR) is used as a metric to check perceptual similarity between the original and reconstructed images. The PSNR value measured in db is tabulated in table 1. According to Chen et al (1998), PSNR above 40 db indicates a good perceptual fidelity. It can be observed that PSNR for the different size of images

TABLE 2
NUMBER OF ITERATIONS MANDATORY TO RECONSTRUCT SHEPP LOGAN PHANTOM

Projections/ Sizes	30	20	15	12	10
64x64	4	4	8	12	18
128x128	10	15	56	58	80
256x256	24	46	124	142	158

TABLE 3
TIME COMPLEXITY OF RECONSTRUCTED PHANTOM IMAGE OF SIZE 64 X 64

Projections/ Cores	30	20	15	12	10
1 Core	1.6495	0.8426	1.3685	1.5327	3.017
2 Core	1.376	0.7431	1.1729	1.4561	2.538
4 Core	0.9769	0.4959	0.9359	1.1558	1.870
8 Core	0.7266	0.4828	0.6749	0.8876	1.453

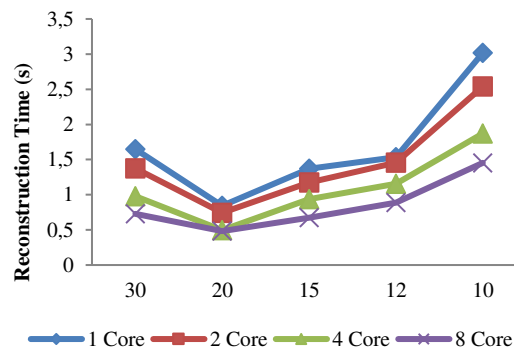


Figure. 13. A graph showing the Time Complexity of reconstructing Phantom image of size 64x 64 sequentially, parallel in 2, 4 and 8 core with respect to projections.

using various angles is above 60 db which indicates the excellent perceptual fidelity.

In figure 11 the PSNR value of the reconstructed image using ART for various sizes in different number of projections is graphed.

Reconstruction time taken by the Algebraic Reconstruction Technique for different size of phantom image in sequential and parallel using 2, 4 and 8 cores in an AMD Processor under LINUX platform. The time complexity of the reconstructed image of various sizes under 2, 4 and 8 cores is given with respect to the number of projections.

Reconstruction time taken by the Algebraic Reconstruction Technique for different size of phantom image in sequential and parallel using 2, 4 and 8 cores in an AMD Processor under LINUX platform. The time complexity of the reconstructed image of various sizes under 2, 4 and 8 cores is given with respect to the number of projections.

TABLE 4
TIME COMPLEXITY OF RECONSTRUCTED PHANTOM
IMAGE OF SIZE 128 X 128

Projections / Cores	30	20	15	12
1 Core	28.8348	32.2032	80.0538	61.2674
2 Core	27.5855	29.6942	70.648	57.9245
4 Core	19.99	22.3794	51.1044	43.9571
8 Core	12.6774	14.533	31.1132	26.7882

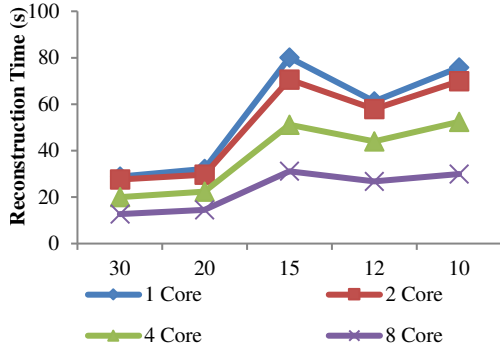


Figure. 14. A graph showing the Time Complexity of reconstructing Phantom image of size 128 x 128 sequentially, parallel in 2, 4 and 8 core with respect to projections

The optimized number of iteration to reconstruct an image in the three represented sizes at 30, 20, 15, 12 and 10 number of projections is tabulated in Table 2 and plotted in figure 12.

In figure 13, 14 and 15 the time complexity of phantom image of size 64, 128 and 256 reconstructed using 2, 4 and 8 cores with respect to 30, 20, 15, 12 and 10 is plotted respectively. Table 3, 4 and 5 tabulates the time complexity for 64, 128 and 256 size images respectively.

Table 3, 4 and 5 shows the reconstruction time taken by 1 Core (row1), 2 core (row2), 4 core (row 3), and 8 core (row 4) when using 30, 20, 15, 12 and 10 projections in the ART for image size 64, 128 and 256 respectively. It is observed that the time gradually reduces as the number of cores increases, for a given sets of projections. A graph is plotted to show the performance of the parallel system. It elucidates the time complexity of the system for a given number of projections using different cores of the parallel processor.

The time complexity of the system implementing parallel processor has got a considerable reduction of time consumptions which is certainly a high degree of utility to the user. A minor change in the time consumption will have a revolutionary impact while it is employed. The specific value of this finding is that the maximum number of core reconstruct the image is fast even for minimum number of projections.

TABLE 5
TIME COMPLEXITY OF RECONSTRUCTED PHANTOM
IMAGE OF SIZE 256 X 256

Projections / Cores	30	20	15	12	10
1 Core	715.2 540	878.7 210	1779 .230 0	1593.5 500	1507.3 800
2 Core	487.6 430	673.5 790	1330 .190 0	1107.0 900	1048.2 700
4 Core	380.0 230	428.8 580	947. 2100	882.23 80	785.83 80
8 Core	218.3 210	254.3 550	503. 6220	495.70 50	414.30 80

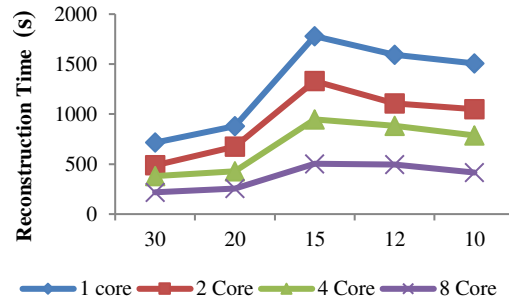


Figure. 15. A graph showing the Time Complexity of reconstructing Phantom image of size 256x256 parallel in 2, 4 and 8 core with respect to projections.

4. Conclusion

The number of iteration mandatory to reconstruct an image is optimized. The images are reconstructed sequentially as well as in parallel environment using different projection data sets. In this study, of Shepp Logan Phantom data is reconstructed using ART and pART. The results have shown encouraging indication of the efficiency of the parallelization of ART algorithm. In general, the pART algorithm gives a paramount computational efficiency better than ART. The computational efficiency of both ART and pART is reported in this article.

References

- [1] R.Murugesan, M.Afeworki, J.A.Cook, N.Devasahayam, R.Tschudin, J.B.Mitchell, S.Subramanian, and M.C.Krishna. A broadband pulsed radio frequency electron paramagnetic resonance spectrometer for biological applications. Review of Scientific Instruments, 69(4), April 1998.
- [2] K.Yamada, R.Murugesan, N.Devasahayam, J.A.Cook, J.B.Mitchell, S.Subramanian, and M.C.Krishna. Evaluation and comparison of

- pulsed and continuous wave radiofrequency electron paramagnetic resonance techniques for in-vivo detection and imaging of free radicals. *Journal of Magnetic Resonance*, 154, 2002.
- [3] R.A.Brooks and G.D.Chiro. *Theory of image reconstruction in computed tomography*. Radiology, 117, December 1975.
- [4] G.L.Zeng. Image reconstruction a tutorial. *Computerized Medical Imaging and Graphics*, 25, 2001.
- [5] P.F.C.Gilbert. Iterative Methods for the three dimensional reconstruction of an object from projections. *Journal of Theory, Biology*, 36, July 1972.
- [6] P.M.V.Subbarao, P.Munshi, and K.Muralidhar. Performance of iterative tomographic algorithms applied to non destructive evaluation with limited data. *NDT and E International*, 30, 1997.
- [7] C.N.Smith and A.D.Stevens. Reconstruction of images from radiofrequency electron paramagnetic resonance spectra. *The British Journal of Radiology*, 67, 1994.
- [8] G.Placidi, M.Alecci, G.Gualtieri, and A.Sotgiu. Optimization of electron paramagnetic resonance image reconstruction using filtered back projection followed by two dimensional deconvolution. *Journal of Magnetic Resonance*, A121, March 1996.
- [9] G.Placidi, M.Alecci, and A.Sotgiu. Fourier reconstruction as a valid alternative to filtered back projection in iterative applications: Implementation of fourier spectral spatial epr imaging. *Journal of Magnetic Resonance*, 134, 1998.
- [10] C.A.Johnson, J.A.Cook, D.McGarry, N.Devasahayam, J.B.Mitchell, S.Subramanian, and M.C.Krishna. Maximum entropy reconstruction methods in electron paramagnetic resonance imaging. *Annals of Operations Research*, 119, January 2003.
- [11] G. T. Herman and A. Lent. Iterative reconstruction algorithms. *Computers in Biology Medicine*, 6, January 1976.
- [12] S.Sivakumar, Murali C.Krishna, R.Murugesan. *Evaluation of Algebraic Iterative Algorithms for Reconstruction of Electron Magnetic Resonance Images*, September 2010.
- [13] Dan Gordon. Parallel ART for image reconstruction in CT using processor arrays. Department of Computer Science, University of Haifa, Haifa 31905, Israel. *The International Journal of Parallel, Emergent and Distributed systems*, Vol. 21, No. 5. October 2006, 365-380. January 2006.
- [14] V. Kumar, A. Grama, A. Gupta, and G. Karayypis, "Introduction to parallel computing: Design and Analysis of Algorithms," Redwood City, Calif.: Benjamin/Cummings, 1994.
- [15] Christopher D.Dharmaraj, Anthony R.Fletcher, Phuc N.Doan, Nallathamby Devasahayam, Shingo MATsumato, Calvin A.Johnson, John A.Cook, James B.Mitchell, Sankaran Subramanian, Murali C.Krishna. Reconstruction for Time-Domain In-Vivo EPR 3-D Multi-Gradient Oximetric Imaging – A Parallel Processing Perspective. Radiation Biology Branch, Center for Cancer Research, National Cancer Institute, NIH, Bethesda, Maryland, USA, 1 June 2009.
- [16] C.Terboven, T.Deselaers, C.Bischof and H.Ney, "Shared-memory parallelization for content-based image retrieval," in ECCV 2006 Workshop on Computation Intensive Methods for Computer Vision, 2006.
- [17] Tiberius Duluman and Constantin Popa, Algebraic Reconstruction Technique versus Conjugate Gradient in Image Reconstruction from Projections, Proceedings of the Fifth Workshop on Mathematical Modelling of Environmental and Life Sciences Problems Constant, Romania, September, 2006, pp. 67–78
- [18] Microslaw Miciak. Radon Transformation and Principle Component Analysis method applied in postal address recognition task. *International Journal of Computer Science and Applications*, Vol 7, No. 3, pp.33 – 44, 2010.
- [19] S. Venturas, I. Flaounas, "Study of Radon Transformation and Application of its Inverse to NMR", Dept. of Informatics & Telecommunications, National and Kapodistrian University of Athens, Paper for "Algorithms in Molecular Biology" Course Assoc. Prof. I. Emiris, 4 July, 2005.
- [20] S.Vandenbergh, Y.D.Asseler, R.Vandewalle. T.Kaupinen, M.Koole, L.Bouwens, K.Laere, I.Lemahieu, and R.A.Direckx. Iterative Reconstruction algorithms in nuclear medicine. *Computerized Medical Imaging and Graphics*, 25, 2001.
- [21] Y. Censor and S. A. Zenios, *Parallel Optimization: Theory, Algorithms, and Applications*, Oxford University Press, New York, NY, USA, 1997.
- [22] S. Kaczmarz, Angenaherte auflosung von systemen linearer gleichungen, *Bulletin de*

- l'Academic Polonaise des Sciences et Lettres, A35 (1937) 355 -357.
- [23] G. T. Herman, *Image Reconstruction from Projections: The Fundamentals of Computerized Tomography*, Academic Press, New York, NY, USA, 1980.
- [24] P. P. B. Eggermont, G. T. Herman and A. Lent, Iterative algorithms for large partitioned linear systems, with applications to image reconstruction, *Linear Algebra and Its Applications*, 40 (1981), pp. 37–67.
- [25] D. Raparia, J. Alessi and A. Kponou. *Algebraic Reconstruction Technique (ART)* AGS Department, Brookhaven National Lab, Upton, NY 11973, USA. Dan Gordon, 1998 IEEE.
- [26] J. S. Kole and F. J. Beekman, “Parallel statistical image reconstruction for cone-beam X-ray CT on a shared memory computation platform,” *Physics in Medicine & Biology*, vol. 50, pp. 1265–1272, 2005.
- [27] C. Soviany, “Embedding data and task parallelism in image processing applications,” Ph.D. dissertation, Technische Univ. Delft, 2003.
- [28] Preeti kaur, Computer Science Department, Guru Nanak Dev University, Amritsar, Punjab, India, “Implementation of Image processing algorithms on the parallel platform using matlab”, *International Journal of Computer Science & Engineering Technology (IJCSET)*.7